

Study of Color Transparency in Production of Vector Mesons off Nuclei¹

J. Nemchik

Institute of Experimental Physics SAS, Watsonova 47, 04353 Kosice, Slovakia

Abstract

Within a light-cone QCD formalism based on the Green function technique incorporating color transparency, coherence length effects and gluon shadowing we study electro-production of vector mesons off nuclei. We found rather large color transparency effects in the range of $Q^2 \leq 10 \div 20 \text{ GeV}^2$. They are stronger at low than at high energies and can be easily identified by HERMES or at JLab. We provide predictions for incoherent and coherent vector meson production for future measurements.

¹Based on the talk presented at the International Conference HADRON STRUCTURE '2002, Herl'any, Slovakia, 22-27 September, 2002.

1 Introduction

One of the fundamental phenomenon coming from the quantum chromodynamics (QCD) is color transparency (CT), which can be treated either in the hadronic or in the quark basis. The former approach leads to Gribov's inelastic corrections [1], the latter one manifests itself as a result of color screening [2, 3]. Although these two approaches are complementary, we will use the quark-gluon interpretation, which is more intuitive and straightforward.

Investigation of diffractive electroproduction of vector mesons off nuclei is very effective for study of CT. A photon of high virtuality Q^2 is expected to produce a pair with a small $\sim 1/Q^2$ transverse separation². Then CT manifests itself as a vanishing absorption of the small sized colorless $\bar{q}q$ wave packet during propagation through the nucleus. Dynamical evolution of the small sized $\bar{q}q$ pair to a normal sized vector meson is controlled by the time scale, called formation time. Due to uncertainty principle, one needs a time interval to resolve different levels V (the ground state) or V' (the next excited state) in the final state. In the rest frame of the nucleus this formation time is Lorentz dilated,

$$t_f = \frac{2 \nu}{m_{V'}^2 - m_V^2} , \quad (1)$$

where ν is the photon energy. A rigorous quantum-mechanical description of the pair evolution was suggested in [4] and is based on the light-cone Green function technique. A complementary description of the same process in the hadronic basis is presented in [5].

Another phenomenon known to cause nuclear suppression is the effect of quantum coherence. It results from destructive interference of the amplitudes for which the interaction takes place on different bound nucleons. Again, it can be estimated by relying on the uncertainty principle and Lorentz time dilation as,

$$t_c = \frac{2 \nu}{Q^2 + m_V^2} . \quad (2)$$

It is usually called coherence time, but we also will use the term coherence length (CL), since light-cone kinematics is assumed, $l_c = t_c$ (similarly, for formation length $l_f = t_f$). CL is related to the longitudinal momentum transfer $q_c = 1/l_c$ in $\gamma^* N \rightarrow V N$, which controls the interference of the production amplitudes from different nucleons.

At high energies (small Bjorken x_{Bj}) gluon shadowing becomes an important phenomenon [6]. It was shown in [6, 7] that for electroproduction of light vector mesons and charmonia off nuclei the gluon shadowing starts to be important at center-of-mass system (c.m.s.) energies $\sqrt{s} \geq 15 \div 30$ GeV and $\sqrt{s} \geq 30 \div 60$ GeV, respectively, depending on nuclear target and Q^2 . Although the gluon shadowing is quite small in the kinematic range important for investigation of CT and discussed in the present paper we include it in all calculations.

In electroproduction of vector mesons off nuclei one needs to disentangle CT (absorption) and CL (shadowing) as the two sources of nuclear suppression. The problem of CT-CL separation arises especially in production of light vector mesons (ρ^0, Φ^0) [6]. In this case the coherence and formation lengths are comparable starting from the photoproduction limit up to $Q^2 \sim 1 \div 2$ GeV². In charmonium production, however, there is a strong inequality $l_f > l_c$

²For production of light vector mesons (ρ^0, Φ^0) very asymmetric pairs can be possible when either q or \bar{q} carries almost the whole photon momentum. As a result the $\bar{q}q$ pair can have a large separation, see Sect. 2 and Eq. (10). However, it is not so for production of charmonia, where mainly symmetric $\bar{q}q$ pairs (either q or \bar{q} carries one half of the whole photon momentum) dominate.

independently of Q^2 and ν [8]. It leads to a different scenario of CT-CL mixing compared to light vector meson production.

Because a variation of l_c with Q^2 can mimic CT at medium and low energies, one can map experimental events in Q^2 and ν in such a way as to keep $l_c = \text{const}$. Then any rise of nuclear transparency, $Tr_A = \sigma(\gamma^* A \rightarrow V X)/A \sigma(\gamma^* N \rightarrow V N)$, with Q^2 would give a signal for CT. We will demonstrate that the LC dipole formalism based on the Green function technique predicts a large effect of CT in the range of $Q^2 \leq 10 \div 20 \text{ GeV}^2$ for both light vector meson [6] and charmonium production [8]. This fact makes it feasible to find a clear signal of CT effects also in exclusive production of vector mesons in the planned future experiments.

Calculations of coherent vector meson production off nuclei show that the effect of CT on the Q^2 dependence of nuclear transparency at $l_c = \text{const}$ is weaker than in the case of incoherent production and is difficult to be detected at low energies since the cross section is small.

2 Light-cone dipole phenomenology for elastic electro-production of vector meson $\gamma^* N \rightarrow V N$.

The light-cone (LC) dipole approach for elastic electroproduction $\gamma^* N \rightarrow V N$ was used in [9, 8] to study the exclusive photo- and electroproduction of charmonia and in [6] for elastic virtual photoproduction of light vector mesons ρ^0 and Φ^0 . Here a diffractive process is treated as elastic scattering of a $\bar{q}q$ fluctuation of the incident particle. The elastic amplitude is given by convolution of the universal flavor independent dipole cross section for the $\bar{q}q$ interaction with a nucleon, $\sigma_{\bar{q}q}$, [2] and the initial and final wave functions. It can be represented in the quantum-mechanical form

$$\mathcal{M}_{\gamma^* N \rightarrow V N}(s, Q^2) = \langle V | \sigma_{\bar{q}q}^N(\vec{r}, s) | \gamma^* \rangle = \int_0^1 d\alpha \int d^2 r \Psi_V^*(\vec{r}, \alpha) \sigma_{\bar{q}q}(\vec{r}, s) \Psi_{\bar{q}q}(\vec{r}, \alpha, Q^2) \quad (3)$$

with the normalization

$$\left. \frac{d\sigma}{dt} \right|_{t=0} = \frac{|\mathcal{M}|^2}{16\pi}. \quad (4)$$

In order to calculate the photoproduction amplitude one needs to know the following ingredients of Eq. (3): (i) the dipole cross section $\sigma_{\bar{q}q}(\vec{r}, s)$ which depends on the $\bar{q}q$ transverse separation \vec{r} and the c.m. energy squared s . (ii) The light-cone (LC) wave function of the $\bar{q}q$ Fock component of the photon $\Psi_{\bar{q}q}(\vec{r}, \alpha, Q^2)$ which also depends on the photon virtuality Q^2 and the relative share α of the photon momentum carried by the quark. (iii) The LC vector meson wave function $\Psi_V(\vec{r}, \alpha)$.

Note that in the LC formalism the photon and meson wave functions contain also higher Fock states $|\bar{q}q\rangle$, $|\bar{q}qG\rangle$, $|\bar{q}q2G\rangle$, etc. The effects of higher Fock states are implicitly incorporated into the energy dependence of the dipole cross section $\sigma_{\bar{q}q}(\vec{r}, s)$ as is given in Eq. (3).

The dipole cross section $\sigma_{\bar{q}q}(\vec{r}, s)$ represents the interaction of a $\bar{q}q$ dipole of transverse separation \vec{r} with a nucleon [2]. It is a flavor independent universal function of \vec{r} and energy and allows to describe various high energy processes in an uniform way. It is known to vanish quadratically $\sigma_{\bar{q}q}(r, s) \propto r^2$ as $r \rightarrow 0$ due to color screening (CT property) and cannot be predicted reliably because of poorly known higher order perturbative QCD (pQCD) corrections and nonperturbative effects. Detailed discussion about the dipole cross section $\sigma_{\bar{q}q}(\vec{r}, s)$ with

an emphasis on the production of light vector mesons is presented in [6]. In electroproduction of charmonia [8] the corresponding transverse separations of $\bar{c}c$ -dipole reach the values ≤ 0.4 fm (semiperturbative region). It means that nonperturbative effects are sufficiently smaller as compared with light vector mesons. Similarly, the relativistic corrections are also small enough and the nonrelativistic limit $\alpha = 0.5$ can be safely used with rather high accuracy [4].

There are two popular parameterizations of $\sigma_{\bar{q}q}(\vec{r}, s)$, GBW presented in [10] and KST suggested in [11]. We choose the second parametrization, because it is valid down to the limit of real photoproduction.

The dipole cross section $\sigma_{\bar{q}q}(\vec{r}, s)$ provides the imaginary part of the elastic amplitude. It is known, however, that the energy dependence of the total cross section generates also a real part [12],

$$\sigma_{\bar{q}q}(r, s) \Rightarrow \left(1 - i \frac{\pi}{2} \frac{\partial}{\partial \ln(s)}\right) \sigma_{\bar{q}q}(r, s). \quad (5)$$

The perturbative distribution amplitude (“wave function”) of the $\bar{q}q$ Fock component of the photon has the following form for transversely (T) and longitudinally (L) polarized photons [13, 14, 15],

$$\Psi_{\bar{q}q}^{T,L}(\vec{r}, \alpha) = \frac{\sqrt{N_C \alpha_{em}}}{2\pi} Z_q \bar{\chi} \hat{O}^{T,L} \chi K_0(\epsilon r) \quad (6)$$

where χ and $\bar{\chi}$ are the spinors of the quark and antiquark, respectively; Z_q is the quark charge, $N_C = 3$ is the number of colors. $K_0(\epsilon r)$ is a modified Bessel function with

$$\epsilon^2 = \alpha(1 - \alpha) Q^2 + m_q^2, \quad (7)$$

where m_q is the quark mass and α is the fraction of the LC momentum of the photon carried by the quark. The operators $\hat{O}^{T,L}$ read,

$$\hat{O}^T = m_q \vec{\sigma} \cdot \vec{e} + i(1 - 2\alpha) (\vec{\sigma} \cdot \vec{n}) (\vec{e} \cdot \vec{\nabla}_r) + (\vec{\sigma} \times \vec{e}) \cdot \vec{\nabla}_r, \quad (8)$$

$$\hat{O}^L = 2Q\alpha(1 - \alpha) (\vec{\sigma} \cdot \vec{n}). \quad (9)$$

Here $\vec{\nabla}_r$ acts on transverse coordinate \vec{r} ; \vec{e} is the polarization vector of the photon, \vec{n} is a unit vector parallel to the photon momentum and $\vec{\sigma}$ is the three vector of the Pauli spin-matrices.

In general, the transverse $\bar{q}q$ separation is controlled by the distribution amplitude Eq. (6) with the mean value,

$$\langle r \rangle \sim \frac{1}{\epsilon} = \frac{1}{\sqrt{Q^2 \alpha(1 - \alpha) + m_q^2}}. \quad (10)$$

For production of light vector mesons very asymmetric $\bar{q}q$ pairs with α or $(1 - \alpha) \lesssim m_q^2/Q^2$ become possible. Consequently, the mean transverse separation $\langle r \rangle \sim 1/m_q$ becomes huge since one must use current quark masses within pQCD. A popular recipe how to fix this problem is to introduce an effective quark mass $m_{eff} \sim \Lambda_{QCD}$ which should represent the nonperturbative interaction effects between q and \bar{q} . However, we introduce this interaction explicitly taking from [11] the corresponding phenomenology based on the light-cone Green function approach.

The Green function $G_{\bar{q}q}(z_1, \vec{r}_1; z_2, \vec{r}_2)$ describes the propagation of an interacting $\bar{q}q$ pair ($\bar{c}c$ pair for the case of J/Ψ production) between points with longitudinal coordinates z_1 and z_2 and

with initial and final separations \vec{r}_1 and \vec{r}_2 . This Green function satisfies the two-dimensional Schrödinger equation,

$$i \frac{d}{dz_2} G_{\bar{q}q}(z_1, \vec{r}_1; z_2, \vec{r}_2) = \left[\frac{\epsilon^2 - \Delta_{r_2}}{2 \nu \alpha (1 - \alpha)} + V_{\bar{q}q}(z_2, \vec{r}_2, \alpha) \right] G_{\bar{q}q}(z_1, \vec{r}_1; z_2, \vec{r}_2) . \quad (11)$$

Here ν is the photon energy. The Laplacian Δ_r acts on the coordinate r .

The imaginary part of the LC potential $V_{\bar{q}q}(z_2, \vec{r}_2, \alpha)$ in (11) is responsible for attenuation of the $\bar{q}q$ in the medium, while the real part represents the interaction between the q and \bar{q} . This potential is supposed to provide the correct LC wave functions of vector mesons. For the sake of simplicity we use the oscillator form of the potential,

$$\text{Re } V_{\bar{q}q}(z_2, \vec{r}_2, \alpha) = \frac{a^4(\alpha) \vec{r}_2^2}{2 \nu \alpha (1 - \alpha)} , \quad (12)$$

which leads to a Gaussian r -dependence of the LC wave function of the meson ground state. The shape of the function $a(\alpha)$ is described in [11] and discussed in [6] for vector meson production.

In this case equation (11) has an analytical solution, the harmonic oscillator Green function [16],

$$\begin{aligned} G_{\bar{q}q}(z_1, \vec{r}_1; z_2, \vec{r}_2) &= \frac{a^2(\alpha)}{2 \pi i \sin(\omega \Delta z)} \exp \left\{ \frac{i a^2(\alpha)}{\sin(\omega \Delta z)} \left[(r_1^2 + r_2^2) \cos(\omega \Delta z) - 2 \vec{r}_1 \cdot \vec{r}_2 \right] \right\} \\ &\times \exp \left[-\frac{i \epsilon^2 \Delta z}{2 \nu \alpha (1 - \alpha)} \right] , \end{aligned} \quad (13)$$

where $\Delta z = z_2 - z_1$ and

$$\omega = \frac{a^2(\alpha)}{\nu \alpha (1 - \alpha)} . \quad (14)$$

The boundary condition is $G_{\bar{q}q}(z_1, \vec{r}_1; z_2, \vec{r}_2)|_{z_2=z_1} = \delta^2(\vec{r}_1 - \vec{r}_2)$.

The probability amplitude to find the $\bar{q}q$ fluctuation of a photon at the point z_2 with separation \vec{r} is given by an integral over the point z_1 where the $\bar{q}q$ is created by the photon with initial zero separation,

$$\Psi_{\bar{q}q}^{T,L}(\vec{r}, \alpha) = \frac{i Z_q \sqrt{\alpha_{em}}}{4 \pi \nu \alpha (1 - \alpha)} \int_{-\infty}^{z_2} dz_1 \left(\bar{\chi} \hat{O}^{T,L} \chi \right) G_{\bar{q}q}(z_1, \vec{r}_1; z_2, \vec{r}) \Big|_{r_1=0} . \quad (15)$$

The operators $\hat{O}^{T,L}$ are defined in Eqs. (8) and (9). Here they act on the coordinate \vec{r}_1 .

If we write the transverse part as

$$\bar{\chi} \hat{O}^T \chi = \bar{\chi} m_q \vec{\sigma} \cdot \vec{e} \chi + \bar{\chi} [i (1 - 2\alpha) (\vec{\sigma} \cdot \vec{n}) \vec{e} + (\vec{\sigma} \times \vec{e})] \chi \cdot \vec{\nabla}_r = E + \vec{F} \cdot \vec{\nabla}_r , \quad (16)$$

then the distribution functions read,

$$\Psi_{\bar{q}q}^T(\vec{r}, \alpha) = Z_q \sqrt{\alpha_{em}} \left[E \Phi_0(\epsilon, r, \lambda) + \vec{F} \vec{\Phi}_1(\epsilon, r, \lambda) \right] , \quad (17)$$

$$\Psi_{\bar{q}q}^L(\vec{r}, \alpha) = 2 Z_q \sqrt{\alpha_{em}} Q \alpha (1 - \alpha) \bar{\chi} \vec{\sigma} \cdot \vec{n} \chi \Phi_0(\epsilon, r, \lambda) , \quad (18)$$

where

$$\lambda = \frac{2 a^2(\alpha)}{\epsilon^2} . \quad (19)$$

The functions $\Phi_{0,1}$ in Eqs. (17) and (18) are defined as

$$\Phi_0(\epsilon, r, \lambda) = \frac{1}{4\pi} \int_0^\infty dt \frac{\lambda}{\text{sh}(\lambda t)} \exp \left[-\frac{\lambda \epsilon^2 r^2}{4} \text{cth}(\lambda t) - t \right], \quad (20)$$

$$\vec{\Phi}_1(\epsilon, r, \lambda) = \frac{\epsilon^2 \vec{r}}{8\pi} \int_0^\infty dt \left[\frac{\lambda}{\text{sh}(\lambda t)} \right]^2 \exp \left[-\frac{\lambda \epsilon^2 r^2}{4} \text{cth}(\lambda t) - t \right]. \quad (21)$$

Note that the $\bar{q} - q$ interaction enters Eqs. (17) and (18) via the parameter λ defined in (19). In the limit of vanishing interaction $\lambda \rightarrow 0$ (i.e. $Q^2 \rightarrow \infty$, α is fixed, $\alpha \neq 0$ or 1) Eqs. (17) - (18) produce the perturbative expressions of Eq. (6). For charmonium production nonperturbative interaction effects are quite weak. Consequently, the parameter λ (19) is rather small due to a large mass of the c quark.

The last ingredient in elastic production amplitude (3) is the vector meson wave function. We use a popular prescription [17] applying the Lorentz boost to the rest frame wave function assumed to be Gaussian which leads to radial parts of transversely and longitudinally polarized mesons in the form,

$$\Phi_V^{T,L}(\vec{r}, \alpha) = C_V^{T,L} \alpha(1 - \alpha) f(\alpha) \exp \left[-\frac{\alpha(1 - \alpha) r^2}{2 R^2} \right] \quad (22)$$

with a normalization defined below, and

$$f(\alpha) = \exp \left[-\frac{m_q^2 R^2}{2 \alpha(1 - \alpha)} \right] \quad (23)$$

with the parameters from [18], $R = 0.183$ fm, $m_q = m_c = 1.5$ GeV for J/Ψ and $R = 0.590$ fm, $m_q = 0.150$ GeV for ρ^0 .

We assume that the distribution amplitude of $\bar{q}q$ fluctuations for vector meson and for the photon have a similar structure [18]. Then in analogy to Eqs. (17) - (18),

$$\Psi_V^T(\vec{r}, \alpha) = (E + \vec{F} \cdot \vec{\nabla}_r) \Phi_V^T(\vec{r}, \alpha); \quad (24)$$

$$\Psi_V^L(\vec{r}, \alpha) = 2 m_V \alpha(1 - \alpha) (\bar{\chi} \vec{\sigma} \cdot \vec{n} \chi) \Phi_V^L(\vec{r}, \alpha). \quad (25)$$

Correspondingly, the normalization conditions for the transverse and longitudinal vector meson wave functions read,

$$N_C \int d^2r \int d\alpha \left\{ m_q^2 \left| \Phi_V^T(\vec{r}, \alpha) \right|^2 + \left[\alpha^2 + (1 - \alpha)^2 \right] \left| \partial_r \Phi_V^T(\vec{r}, \alpha) \right|^2 \right\} = 1 \quad (26)$$

$$4 N_C \int d^2r \int d\alpha \alpha^2 (1 - \alpha)^2 m_V^2 \left| \Phi_V^L(\vec{r}, \alpha) \right|^2 = 1. \quad (27)$$

3 Electroproduction of vector mesons on a nucleon

The forward production amplitude $\gamma^* N \rightarrow V N$ for transverse and longitudinal photons and vector mesons is calculated using the nonperturbative photon Eqs. (17), (18) and vector meson

Eqs. (24), (25) wave functions and has the following form,

$$\begin{aligned} \mathcal{M}_{\gamma^* N \rightarrow VN}^T(s, Q^2) \Big|_{t=0} &= N_C Z_q \sqrt{2 \alpha_{em}} \int d^2 r \sigma_{\bar{q}q}(\vec{r}, s) \int_0^1 d\alpha \left\{ m_q^2 \Phi_0(\epsilon, \vec{r}, \lambda) \Phi_V^T(\vec{r}, \alpha) \right. \\ &\quad \left. - [\alpha^2 + (1 - \alpha)^2] \vec{\Phi}_1(\epsilon, \vec{r}, \lambda) \cdot \vec{\nabla}_r \Phi_V^T(\vec{r}, \alpha) \right\}; \end{aligned} \quad (28)$$

$$\begin{aligned} \mathcal{M}_{\gamma^* N \rightarrow VN}^L(s, Q^2) \Big|_{t=0} &= 4 N_C Z_q \sqrt{2 \alpha_{em}} m_V Q \int d^2 r \sigma_{\bar{q}q}(\vec{r}, s) \\ &\quad \times \int_0^1 d\alpha \alpha^2 (1 - \alpha)^2 \Phi_0(\epsilon, \vec{r}, \lambda) \Phi_V^L(\vec{r}, \alpha). \end{aligned} \quad (29)$$

These amplitudes are normalized as $|\mathcal{M}^{T,L}|^2 = 16\pi d\sigma_N^{T,L}/dt \Big|_{t=0}$. The real part of the amplitude is included according to the prescription described in the previous section. We calculate the cross sections $\sigma = \sigma^T + \epsilon' \sigma^L$ assuming that the photon polarization is $\epsilon' = 1$.

We checked in [6] and [8] the absolute value of the production cross section by comparing with data for elastic electroproduction of light vector mesons and charmonia. We found a good agreement of the model predictions with the data on the Q^2 dependence of the cross section. As the second test of our approach we compared also the model calculations with the data on the real vector meson photoproduction [6, 8]. Successful description of those data confirms an importance (especially for light vector mesons) of the nonperturbative interaction effects between the q and \bar{q} included into calculations.

As a cross-check for the choice of the vector meson wave function in Eqs. (22) and (23) we also calculated the total V -nucleon cross section, which has the following form,

$$\sigma_{tot}^{VN} = N_C \int d^2 r \int d\alpha \left\{ m_q^2 \left| \Phi_V^T(\vec{r}, \alpha) \right|^2 + [\alpha^2 + (1 - \alpha)^2] \left| \partial_r \Phi_V^T(\vec{r}, \alpha) \right|^2 \right\} \sigma_{\bar{q}q}(\vec{r}, s) \quad (30)$$

At $\sqrt{s} = 10$ GeV we obtain [8] $\sigma_{tot}^{J/\Psi N} = 4.2$ mb which is not in contradiction with $\sigma_{tot}^{J/\Psi N} = 3.6 \pm 0.1$ mb evaluated in [9] using more realistic $\bar{q} - q$ potentials and/or charmonium wave functions. For ρ^0 we obtained [6] $\sigma_{tot}^{\rho N} = 26.5$ mb, which is very close to pion-nucleon total cross section.

4 Incoherent production of vector mesons off nuclei

In diffractive incoherent (quasielastic) production of vector mesons off nuclei, $\gamma^* A \rightarrow V X$, one sums over all final states of the target nucleus except those which contain particle (pion) creation. The observable usually studied experimentally is nuclear transparency defined as

$$Tr_A^{inc} = \frac{\sigma_{\gamma^* A \rightarrow VX}^{inc}}{A \sigma_{\gamma^* N \rightarrow VN}}. \quad (31)$$

The t -slope of the differential quasielastic cross section is the same as on a nucleon target. Therefore, instead of integrated cross sections one can also use nuclear transparency expressed via the forward differential cross sections Eq. (4),

$$Tr_A^{inc} = \frac{1}{A} \left| \frac{\mathcal{M}_{\gamma^* A \rightarrow VX}(s, Q^2)}{\mathcal{M}_{\gamma^* N \rightarrow VN}(s, Q^2)} \right|^2. \quad (32)$$

In the LC Green function approach [6] the physical photon $|\gamma^*\rangle$ is decomposed into different Fock states, namely, the bare photon $|\gamma^*\rangle_0$, $|\bar{q}q\rangle$, $|\bar{q}qG\rangle$, etc. As we mentioned above the higher Fock states containing gluons describe the energy dependence of the photoproduction reaction on a nucleon. Besides, those Fock components also lead to gluon shadowing as far as nuclear effects are concerned. However, these fluctuations are heavier and have a shorter coherence time (lifetime) than the lowest $|\bar{q}q\rangle$ state. Therefore, at medium energies only $|\bar{q}q\rangle$ fluctuations of the photon matter. Consequently, gluon shadowing related to the higher Fock states will be dominated at high energies. Detailed description and calculation of gluon shadowing for the case of vector meson production off nuclei is presented in [6, 7]. Although the gluon shadowing effects are rather small in the kinematic range important for study of CT effects we include them in all calculations.

Propagation of an interacting $\bar{q}q$ pair in a nuclear medium is also described by the Green function satisfying the evolution Eq. (11). However, the potential in this case acquires an imaginary part which represents absorption in the medium,

$$ImV_{\bar{q}q}(z_2, \vec{r}, \alpha) = -\frac{\sigma_{\bar{q}q}(\vec{r}, s)}{2} \rho_A(b, z_2), \quad (33)$$

where $\rho_A(b, z_2)$ is the nuclear density function defined at the point with longitudinal coordinate z_2 and impact parameter \vec{b} .

The analytical solution of Eq. (13) is only known for the harmonic oscillator potential $V(r) \propto r^2$. To keep the calculations reasonably simple we are forced to use the dipole approximation

$$\sigma_{\bar{q}q}(r, s) = C(s) r^2, \quad (34)$$

which allows to obtain the Green function in an analytical form. The energy dependent factor $C(s)$ in Eq. (34) is adjusted by the procedure described in [6].

With the potential Eqs. (33) – (34) the solution of Eq. (11) has the same form as Eq. (13), except that one should replace $\omega \Rightarrow \Omega$ and $a^2(\alpha) \Rightarrow b(\alpha)$, where

$$\Omega = \frac{b(\alpha)}{\nu \alpha(1-\alpha)} = \frac{\sqrt{a^4(\alpha) - i \rho_A(b, z) \nu \alpha (1-\alpha) C(s)}}{\nu \alpha(1-\alpha)}. \quad (35)$$

As we discussed in [6] the value of l_c can distinguish different regimes of vector meson production.

(i) The CL is much shorter than the mean nucleon spacing in a nucleus ($l_c \rightarrow 0$). For light vector mesons $l_f \sim l_c$ and consequently $l_f \rightarrow 0$ as well. In this case $G(z_2, \vec{r}_2; z_1, \vec{r}_1) \rightarrow \delta(z_2 - z_1)$. Tr_A^{inc} is given by the simple formula corresponding to the Glauber approximation [6, 8].

(ii) In production of charmonia and other heavy flavor quarkonii there is a strong inequality $l_c < l_f$ and the intermediate case $l_c \rightarrow 0$, but $l_f \sim R_A$ (R_A is the nuclear radius) can be realized. Then the formation of the meson wave function is described by the Green function and the numerator of the nuclear transparency ratio Eq. (32) has the form [4],

$$\left| \mathcal{M}_{\gamma^* A \rightarrow V X}(s, Q^2) \right|_{l_c \rightarrow 0; l_f \sim R_A}^2 = \int d^2 b \int_{-\infty}^{\infty} dz \rho_A(b, z) \left| F_1(b, z) \right|^2, \quad (36)$$

where

$$F_1(b, z) = \int_0^1 d\alpha \int d^2 r_1 d^2 r_2 \Psi_V^*(\vec{r}_2, \alpha) G(z', \vec{r}_2; z, \vec{r}_1) \sigma_{\bar{q}q}(r_1, s) \Psi_{\bar{q}q}(\vec{r}_1, \alpha) \Big|_{z' \rightarrow \infty} \quad (37)$$

(iii) In the high energy limit, the CL $l_c \gg R_A$. In this case $G(z_2, \vec{r}_2; z_1, \vec{r}_1) \rightarrow \delta(\vec{r}_2 - \vec{r}_1)$, i.e. all fluctuations of the transverse $\bar{q}q$ separation are “frozen” by Lorentz time dilation. Then, the numerator on the r.h.s. of Eq. (32) takes the form [4],

$$\left| \mathcal{M}_{\gamma^* A \rightarrow V X}(s, Q^2) \right|_{l_c \gg R_A}^2 = \int d^2 b T_A(b) \left| \int d^2 r \int_0^1 d\alpha \right. \\ \times \Psi_V^*(\vec{r}, \alpha) \sigma_{\bar{q}q}(r, s) \exp \left[-\frac{1}{2} \sigma_{\bar{q}q}(r, s) T_A(b) \right] \Psi_{\bar{q}q}(\vec{r}, \alpha, Q^2) \left. \right|^2, \quad (38)$$

where $T_A(b) = \int_{-\infty}^{\infty} dz \rho_A(b, z)$ is the nuclear thickness function.

(iv) This regime reflects the general case when there is no restrictions for either l_c or l_f . The corresponding theoretical tool has been developed for the first time in [6]. In this general case the incoherent photoproduction amplitude is represented as a sum of two terms [19],

$$\left| \mathcal{M}_{\gamma^* A \rightarrow V X}(s, Q^2) \right|^2 = \int d^2 b \int_{-\infty}^{\infty} dz \rho_A(b, z) \left| F_1(b, z) - F_2(b, z) \right|^2. \quad (39)$$

The first term $F_1(b, z)$ introduced above in Eq. (37) alone would correspond to the short l_c limit (ii). The second term $F_2(b, z)$ in Eq. (39) corresponds to the situation when the incident photon produces a $\bar{q}q$ pair diffractively and coherently at the point z_1 prior to incoherent quasielastic scattering at point z . The LC Green functions describe the evolution of the $\bar{q}q$ over the distance from z_1 to z and further on, up to the formation of the meson wave function. Correspondingly, this term has the form,

$$F_2(b, z) = \frac{1}{2} \int_{-\infty}^z dz_1 \rho_A(b, z_1) \int_0^1 d\alpha \int d^2 r_1 d^2 r_2 d^2 r \Psi_V^*(\vec{r}_2, \alpha) \\ \times G(z' \rightarrow \infty, \vec{r}_2; z, \vec{r}) \sigma_{\bar{q}q}(\vec{r}, s) G(z, \vec{r}; z_1, \vec{r}_1) \sigma_{\bar{q}q}(\vec{r}_1, s) \Psi_{\bar{q}q}(\vec{r}_1, \alpha). \quad (40)$$

Eq. (39) correctly reproduces the limits (i) - (iii).

Exclusive incoherent electroproduction of vector mesons off nuclei has been suggested in [20] for investigation of CT. Increasing the photon virtuality Q^2 one squeezes the produced $\bar{q}q$ wave packet. Such a small colorless system propagates through the nucleus with little attenuation, provided that the energy is sufficiently high ($l_f \gg R_A$) so the fluctuations of the $\bar{q}q$ separation are frozen during propagation. Consequently, a rise of nuclear transparency $Tr_A^{inc}(Q^2)$ with Q^2 should give a signal for CT. Indeed, such a rise was observed in the E665 experiment [21] at Fermilab for exclusive production of ρ^0 mesons off nuclei what has been claimed as manifestation of CT.

However, the effect of coherence length [22, 23] leads also to a rise of $Tr_A^{inc}(Q^2)$ with Q^2 and so can imitate CT effects. This happens when the coherence length varies from long to short (see Eq. (2)) compared to the nuclear size and the length of the path in nuclear matter becomes shorter. Consequently, the vector meson (or $\bar{q}q$) attenuates less in nuclear medium. This happens when Q^2 increases at fixed ν . Therefore one should carefully disentangle these two phenomena.

Model calculations of incoherent ρ and J/Ψ production off nuclei were tested in comparison with available data and a nice agreement has been found [6, 8]. However, the available data do not solve the problem of separation of CT and CL effects discussed in [6]. Because of $l_c \gtrsim l_f$ at

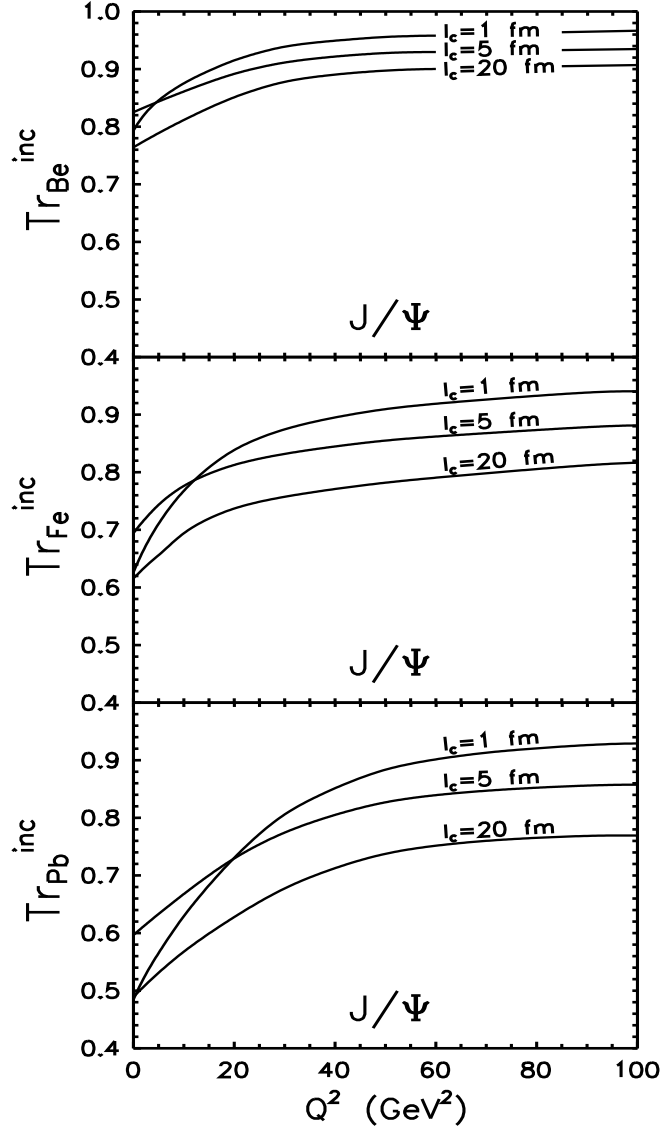


Figure 1: Q^2 dependence of the nuclear transparency Tr_A^{inc} for exclusive electroproduction of J/Ψ on nuclear targets ${}^9\text{Be}$, ${}^{56}\text{Fe}$ and ${}^{207}\text{Pb}$ (from top to bottom). The CL is fixed at $l_c = 1, 5$ and 20 fm .

$Q^2 \lesssim 1 \div 2 \text{ GeV}^2$ for production of ρ^0 and Φ^0 [6] and a strong inequality $l_c < l_f$ for charmonium production [8], there is a different scenario of CT-CL mixing for light and heavy vector mesons production.

In order to eliminate the effect of CL from the data on the Q^2 dependence of nuclear transparency one should simply bin the data in a such way which keeps $l_c = \text{const}$ [5]. It means that one should vary simultaneously ν and Q^2 maintaining the CL Eq. (2) constant,

$$\nu = \frac{1}{2} l_c (Q^2 + m_V^2) . \quad (41)$$

In this case the Glauber model predicts a Q^2 independent nuclear transparency, and any rise with Q^2 would signal CT [5].

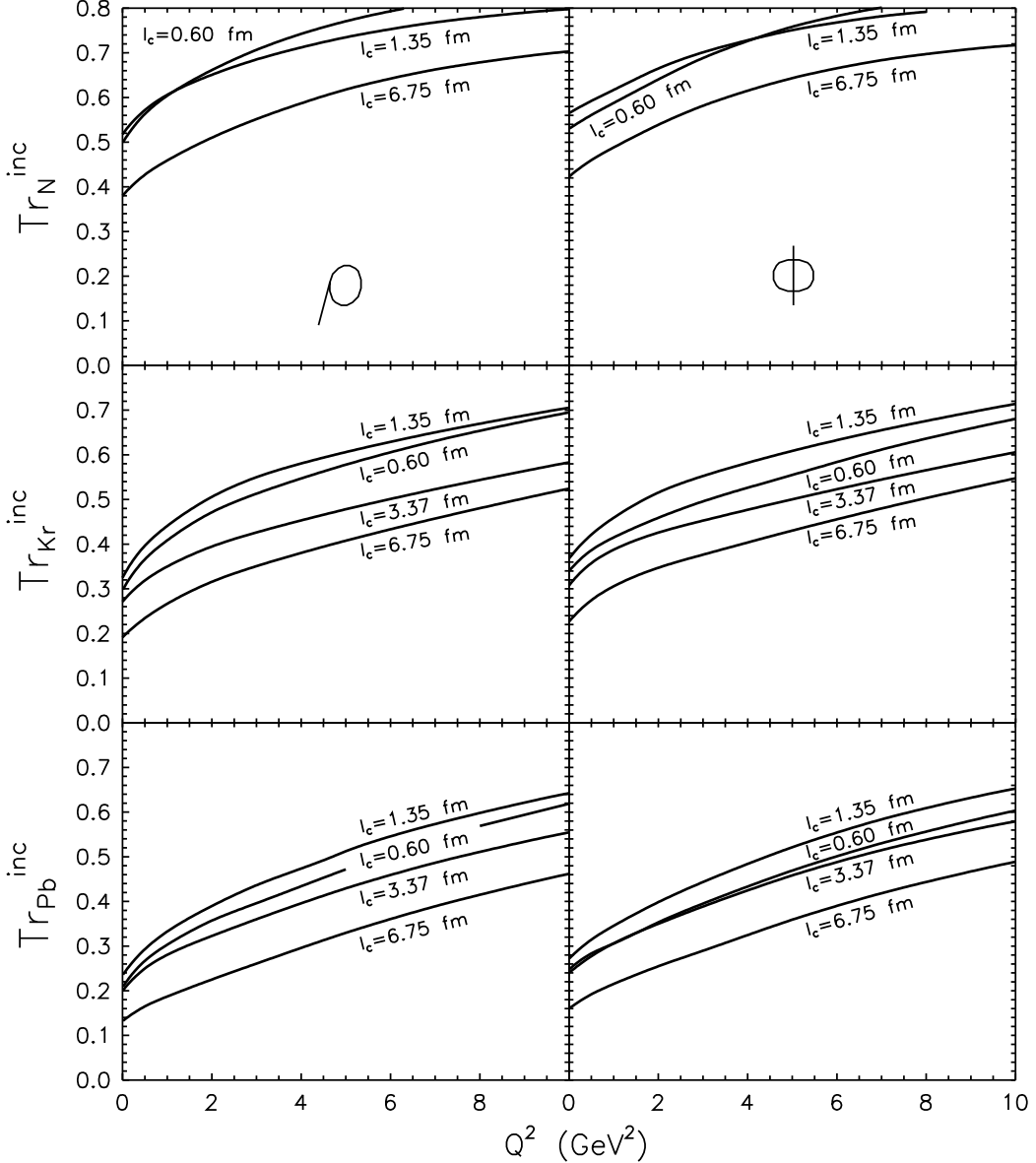


Figure 2: Q^2 dependence of the nuclear transparency Tr_A^{inc} for exclusive electroproduction of ρ (left) and Φ (right) mesons on nuclear targets ^{14}N , ^{84}Kr and ^{207}Pb (from top to bottom). The CL is fixed at $l_c = 0.60, 1.35, 3.37$ and 6.75 fm.

The LC Green function technique incorporates both the effects of coherence and formation. We performed calculations of $Tr_A^{inc}(Q^2)$ at fixed l_c starting from different minimal values of ν , which correspond to real photoproduction in Eq. (41),

$$\nu_{min} = \frac{1}{2} l_c m_V^2 . \quad (42)$$

The results for incoherent production of J/Ψ at $\nu_{min} = 24.3, 121.7$ and 487 GeV ($l_c = 1, 5$ and 20 fm) are presented in Fig. 1 for beryllium, iron and lead. We use the nonperturbative LC wave function of the photon with the parameters of the LC potential described in [8]. We use quark mass $m_q = m_c = 1.5$ GeV.

The analogical results for incoherent production of ρ and Φ mesons at $l_c = 0.60, 1.35, 3.37$ and 6.75 fm are presented in Fig. 2 for nitrogen, krypton and lead.

The both Figs. 1 and 2 exhibit large CT effects. Although the predicted Q^2 - variation of nuclear transparency at fixed l_c for J/Ψ is less than for light vector mesons, it is still sufficiently significant to be investigated experimentally even in the range of $Q^2 \lesssim 20$ GeV 2 . CT effects (the rise with Q^2 of nuclear transparency) are more pronounced at low than at high energies and can be easily identified by the planned future experiments.

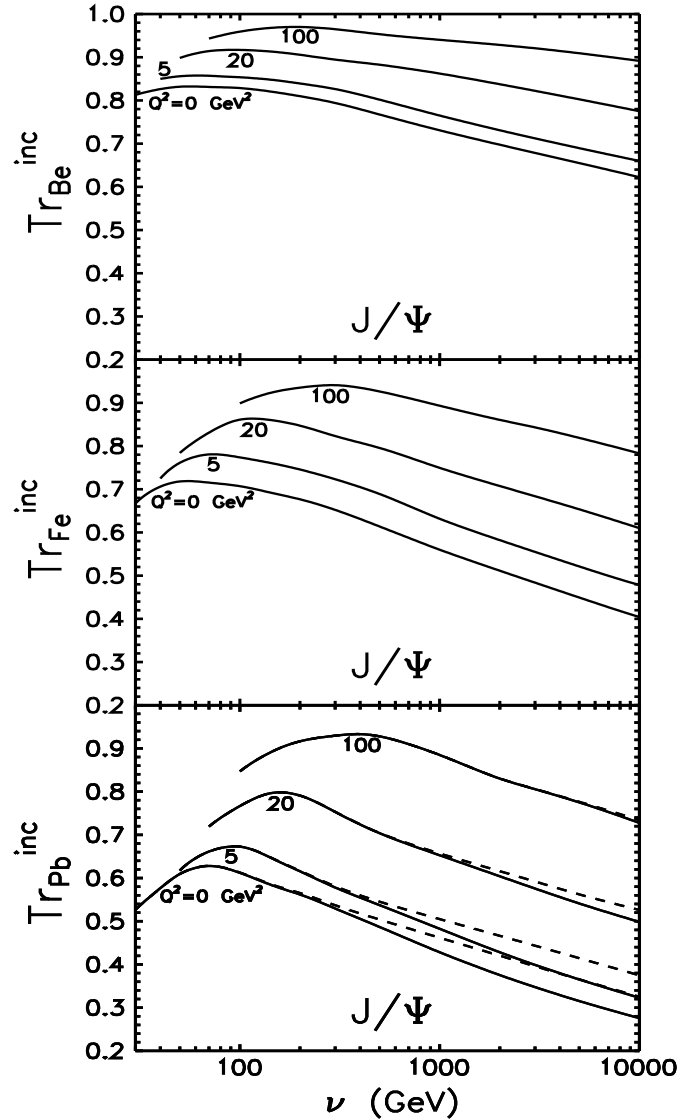


Figure 3: Nuclear transparency for incoherent electroproduction $\gamma^* A \rightarrow J/\Psi X$ as function of energy at $Q^2 = 0, 5, 20$ and 100 GeV 2 for beryllium, iron and lead. The solid curves and dashed curves for lead correspond to calculations with and without gluon shadowing, respectively.

We also calculated the energy dependence of nuclear transparency for charmonium production [8] at fixed Q^2 (analogical Fig. for light vector meson production can be found in [6]). The results for beryllium, iron and lead are shown in Fig. 3 for different values of Q^2 . The

interesting feature is the presence of a maximum of transparency at some energy which is much more evident than in production of light vector mesons [6]. At small and moderate energies a strong rise of Tr_A^{inc} with energy especially for the lead target is a manifestation of net CT effects resulting from a strong inequality $l_c < l_f$. The existence of maxima of Tr_A^{inc} results from the interplay of coherence and formation effects. Indeed, the formation length rises with energy leading to an increasing nuclear transparency. At some energy, however, the effect of CL is switched on leading to a growth of the path length of the $\bar{q}q$ in the nucleus, i.e. to a suppression of nuclear transparency. This also explains the unusual ordering of curves at small and moderate Q^2 calculated for different values of l_c as is depicted in Fig. 1.

5 Coherent production of vector mesons

In general, in coherent (elastic) electroproduction of a vector mesons the target nucleus remains intact, so all the vector mesons produced at different longitudinal coordinates and impact parameters add up coherently. This condition considerably simplifies the expressions for the production cross sections. The integrated cross section has the form,

$$\sigma_A^{coh} \equiv \sigma_{\gamma^* A \rightarrow VA}^{coh} = \int d^2 q \left| \int d^2 b e^{i \vec{q} \cdot \vec{b}} \mathcal{M}_{\gamma^* A \rightarrow VA}^{coh}(b) \right|^2 = \int d^2 b |\mathcal{M}_{\gamma^* A \rightarrow VA}^{coh}(b)|^2 , \quad (43)$$

where

$$\mathcal{M}_{\gamma^* A \rightarrow VA}^{coh}(b) = \int_{-\infty}^{\infty} dz \rho_A(b, z) F_1(b, z) , \quad (44)$$

with the function $F_1(b, z)$ defined in Eq. (37).

One should not use Eq. (32) for nuclear transparency any more since the t -slopes of the differential cross sections for nucleon and nuclear targets are different and do not cancel in the ratio. Therefore, the nuclear transparency also includes the slope parameter B_V for the process $\gamma^* N \rightarrow V N$,

$$Tr_A^{coh} = \frac{\sigma_A^{coh}}{A \sigma_N} = \frac{16 \pi B_V \sigma_A^{coh}}{A |\mathcal{M}_{\gamma^* N \rightarrow VN}(s, Q^2)|^2} . \quad (45)$$

One can eliminate the effects of CL and single out the net CT effect in a way similar to what was suggested for incoherent reactions by selecting experimental events with $l_c = const$. We calculated nuclear transparency for the coherent reaction $\gamma^* A \rightarrow J/\Psi A$ at fixed values of l_c . The results for $l_c = 1, 5$ and 20 fm are depicted in Fig. 4 for several nuclei. We performed calculations of Tr_A^{coh} with the slope $B_V = B_{J/\Psi} = 4.7 \text{ GeV}^{-2}$. The effect of a rise of Tr_A^{coh} is not sufficiently large to be observable in the range of $Q^2 \leq 20 \text{ GeV}^2$. A wider range of $Q^2 \leq 100 \text{ GeV}^2$ and heavy nuclei gives higher chances for experimental investigation of CT. However, on the other hand, it encounters the problem of low yields at high Q^2 .

We calculated also nuclear transparency for coherent production of light vector mesons at fixed values of l_c . We took parametrization of the slope parameter from [6]. The results for $l_c = 1.35, 3.37$ and 13.50 fm are presented in Fig. 5 [6].

Note that in contrast to incoherent production where nuclear transparency is expected to saturate as $Tr_A^{inc}(Q^2) \rightarrow 1$ at large Q^2 , for the coherent process nuclear transparency reaches a higher limit, $Tr_A^{coh}(Q^2) \rightarrow A^{1/3}$.

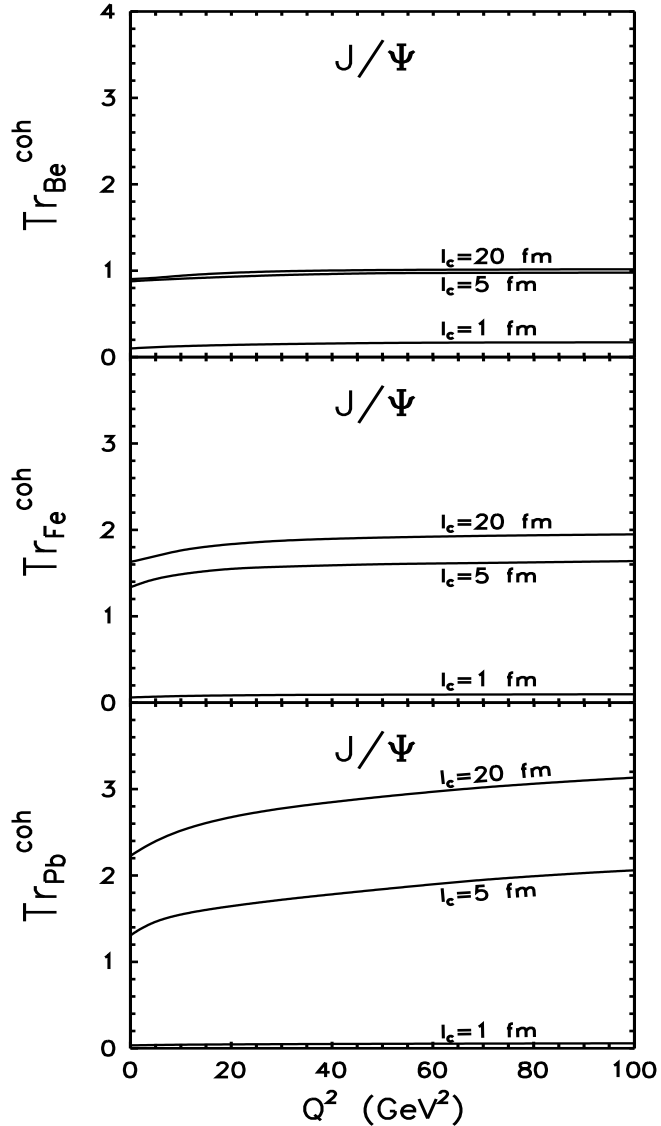


Figure 4: The same as in Fig. 1, but for coherent production of J/Ψ , $\gamma^* A \rightarrow J/\Psi A$.

We also calculated nuclear transparency as function of energy at fixed Q^2 . The results for J/Ψ produced coherently off beryllium, iron and lead are depicted in Fig. 6 at $Q^2 = 0, 5, 20$ and 100 GeV^2 (analogical Fig. for coherent production of light vector mesons can be found in [6]). At low energy, Tr_A^{coh} is very small due to suppression of the nuclear coherent cross section by the nuclear form factor. The reason is that the longitudinal momentum transfer, which is equal to the inverse CL, is large when the CL is short. At high energy, however, $l_c \gg R_A$ and nuclear transparency nearly saturates (it decreases with ν only due to the rising dipole cross section). The saturation level is higher at larger Q^2 which is a manifestation of CT.

Note that in all calculations the effects of gluon shadowing are included in a way analogical to that described in the recent papers [6, 7]. For illustration they are depicted in Figs. 3 and 6 for the lead target as a difference between solid and dashed lines at various values of Q^2 . For charmonium production, in the photoproduction limit $Q^2 = 0$ the onset of gluon

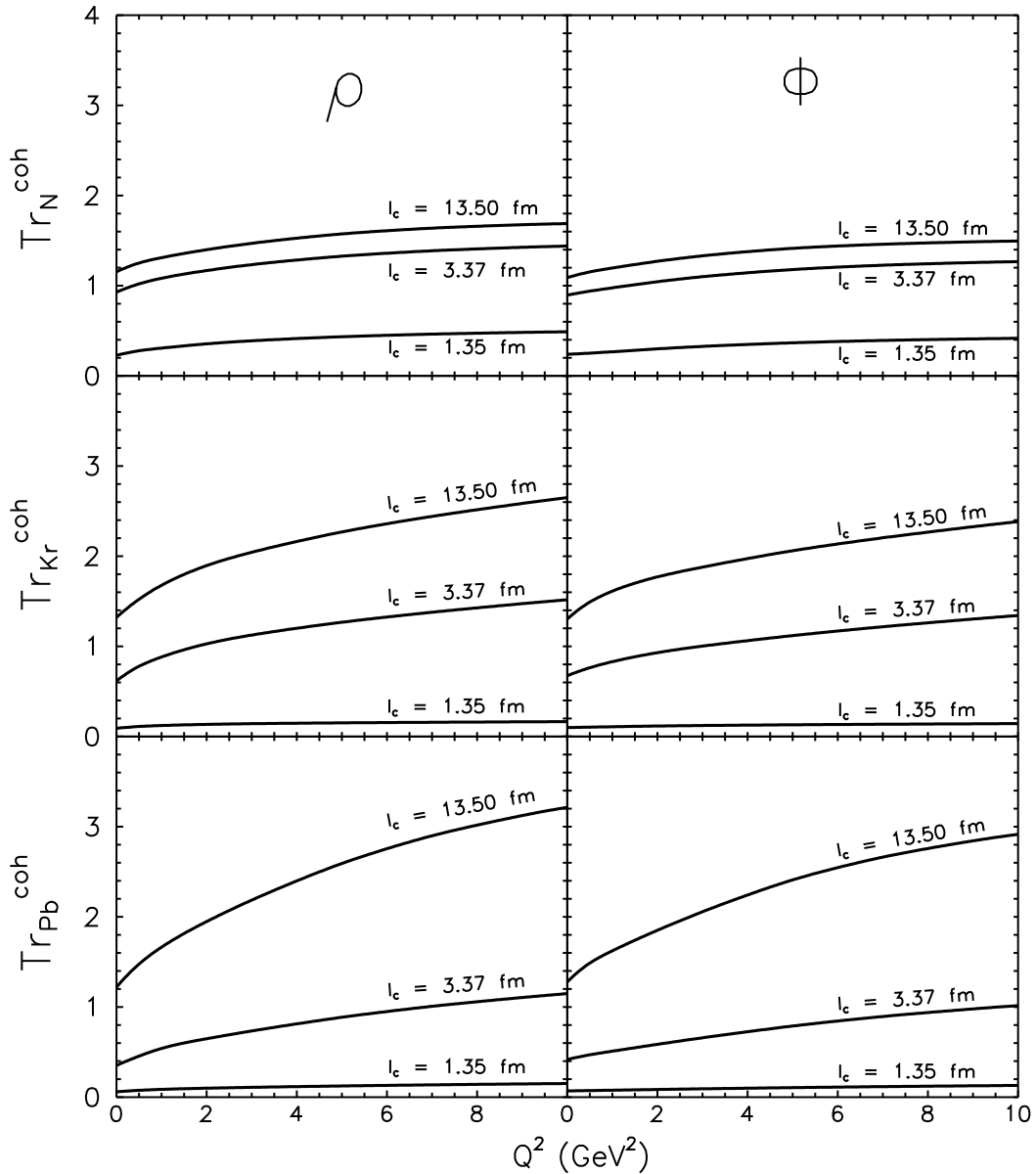


Figure 5: The same as in Fig. 2, but for coherent production of ρ and Φ , $\gamma^* A \rightarrow V A$.

shadowing becomes important at rather high photon energy $\nu > 1000$ GeV for incoherent and $\nu > 500$ GeV for coherent production. In the production of light vector mesons [6], however, the onset of gluon shadowing is important at much smaller energies due to much smaller masses of $\bar{q}q$ fluctuations of the photon. This corresponds to the claim made in [11] that the onset of gluon shadowing requires smaller x_{Bj} than the onset of quark shadowing. The reason is that the fluctuations containing gluons are in general heavier than the $\bar{q}q$ and have a shorter CL.

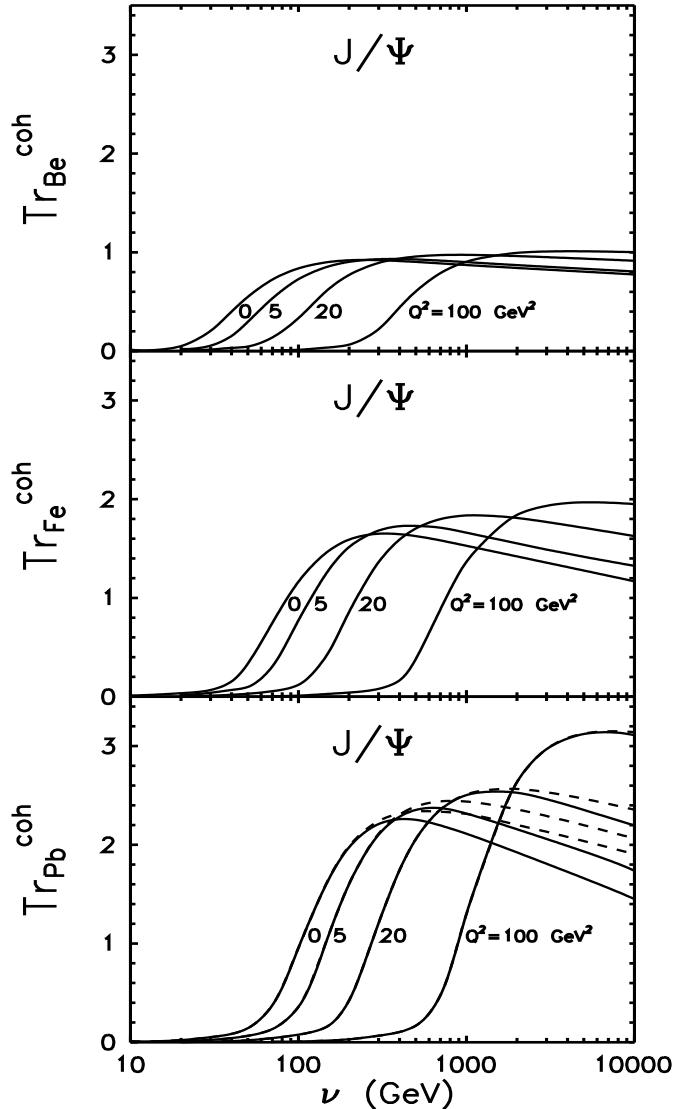


Figure 6: Nuclear transparency for coherent electroproduction $\gamma^* A \rightarrow J/\Psi A$ as function of energy at $Q^2 = 0, 5, 20$ and 100 GeV^2 for beryllium, iron and lead. The solid curves and dashed curves for lead correspond to calculations with and without gluon shadowing, respectively.

6 Summary and conclusions

We presented a rigorous quantum-mechanical approach based on the light-cone QCD Green function formalism which naturally incorporates the interference effects of CT and CL. Within this approach [8, 6] we studied CT effects in coherent and incoherent electroproduction of light vector mesons and charmonia off nuclei.

The onset of coherence effects (shadowing) can mimic the expected signal of CT in incoherent electroproduction of vector mesons at medium and large energies. In order to single out the formation effect the data must be taken at such energy and Q^2 which keep $l_c = \text{const.}$ Then the observation of a rise with Q^2 of nuclear transparency for fixed l_c would give a signal of color

transparency. Predictions of $Tr_A^{inc}(Q^2)$ as a function of Q^2 at different fixed l_c show rather large CT effects in incoherent production of light vector mesons and charmonia. Although for charmonium production [8] the Q^2 - variation of nuclear transparency at fixed l_c is predicted to be less than for the production of light vector mesons [6], it is still sufficiently significant to be investigated experimentally even in the range of $Q^2 \lesssim 10 \div 20 \text{ GeV}^2$. CT effects (the rise with Q^2 of nuclear transparency) are more pronounced at low than at high energies and can be easily identified by HERMES and planned future experiments.

The effects of CT in coherent production of vector mesons are found to be less pronounced. A wider range $Q^2 \leq 100 \text{ GeV}^2$ and heavy nuclei give higher chances for experimental investigation of CT. However, on the other hand, it faces the problem of low yields at high Q^2 .

Nuclear suppression of gluons was calculated within the same LC approach and included in predictions. It was manifested that these corrections are quite small at medium energies which are dominant in the process of searching for CT effects.

Concluding, the predicted large effects of CT in electroproduction of light vector mesons and charmonia off nuclei open further possibilities to search for CT with medium energy electrons and can be tested at HERMES and in future experiments.

Acknowledgments: This work has been supported in part by the Slovak Funding Agency, Grant No. 2/2099/22.

References

- [1] V.N. Gribov, Sov. Phys. JETP **29**, 483 (1969).
- [2] A.B. Zamolodchikov, B.Z. Kopeliovich and L.I. Lapidus, Sov. Phys. JETP Lett. **33**, 595 (1981).
- [3] G. Bertsch, S.J. Brodsky, A.S. Goldhaber and J.F. Gunion, Phys. Rev. Lett. **47**, 297 (1981).
- [4] B.Z. Kopeliovich and B.G. Zakharov, Phys. Rev. D **44**, 3466 (1991).
- [5] J. Hüfner and B.Z. Kopeliovich, Phys. Lett. B **403**, 128 (1997).
- [6] B.Z. Kopeliovich, J. Nemchik, A. Schaefer and A.V. Tarasov, Phys. Rev. C **65**, 035201 (2002).
- [7] Yu.P. Ivanov, B.Z. Kopeliovich, A.V. Tarasov and J. Huefner, Phys. Rev. C **66**, 024903 (2002).
- [8] J. Nemchik, Phys. Rev. C **66**, 045204 (2002).
- [9] J. Huefner, Yu.P. Ivanov, B.Z. Kopeliovich and A.V. Tarasov, Phys. Rev. D **62**, 094022 (2000)
- [10] K. Golec-Biernat and M. Wüsthoff, Phys. Rev. D **59**, 014017 (1999); Phys. Rev. D **60**, 114023 (1999).
- [11] B.Z. Kopeliovich, A. Schäfer and A.V. Tarasov, Phys. Rev. D **62**, 054022 (2000).

- [12] J.B. Bronzan, G.L. Kane and U.P. Sukhatme, Phys. Lett. B **49**, 272 (1974).
- [13] J.B. Kogut and D.E. Soper, Phys. Rev. D **1**, 2901 (1970).
- [14] J.M. Bjorken, J.B. Kogut and D.E. Soper, Phys. Rev. D **3**, 1382 (1971).
- [15] N.N. Nikolaev and B.G. Zakharov, Z. Phys. C **49**, 607 (1991).
- [16] R.P. Feynman and A.R. Gibbs, *Quantum Mechanics and Path Integrals* (McGraw-Hill, New York, 1965).
- [17] M.V. Terent'ev, Sov. J. Nucl. Phys. **24**, 106 (1976).
- [18] J. Nemchik, N.N. Nikolaev, E. Predazzi and B.G. Zakharov, Z. Phys. C **75**, 71 (1997).
- [19] J. Hüfner, B.Z. Kopeliovich and A. Zamolodchikov, Z. Phys. A **357**, 113 (1997).
- [20] B.Z. Kopeliovich, J. Nemchik, N.N. Nikolaev and B.G. Zakharov, Phys. Lett. B **324**, 469 (1994).
- [21] E665 Collaboration, M.R. Adams et al., Phys. Rev. Lett. **74**, 1525 (1995).
- [22] B.Z. Kopeliovich and J. Nemchik, nucl-th/9511018.
- [23] J. Hüfner, B.Z. Kopeliovich and J. Nemchik, Phys. Lett. B **383**, 362 (1996).